Journal of Physiology (1991), **434**, *pp.* 121–149
With 18 figures
Printed in Great Britain

ON THE SODIUM AND POTASSIUM CURRENTS OF A HUMAN NEUROBLASTOMA CELL LINE

BY B. L. GINSBORG, R. J. MARTIN* AND L. PATMORE†

*From the Department of Pharmacology and *Preclinical Veterinary Sciences, University of Edinburgh and †Department of Pharmacology, Syntex Research Centre, Edinburgh*

(*Received 19 April 1990*)

SUMMARY

1. The patch-clamp method was applied to the study of ionic currents activated by depolarization of undifferentiated IMR-32 human neuroblastoma cells. Whole-cell sodium and potassium currents and single potassium ion channel currents from cell-attached patches were investigated.

2. Cells had a mean resting potential of −38 mV and mean input resistance of 1·6 GΩ. Single action potentials were evoked under current clamp during the injection of depolarizing currents.

3. A voltage-dependent inward sodium current was observed which reversed at +44 mV. A Boltzmann fit to the activation curve gave a half-maximal activation voltage of −41·6 mV and a 'slope' of 3·9 mV. The steady-state inactivation curve had a half-maximal inactivation voltage of −81 mV and a 'slope' of 9·7 mV.

4. The time-dependent activation and inactivation of the current displayed classical Hodgkin–Huxley kinetics. Values for the time constants τ_m and τ_h of 0·16 and 0·63 ms were calculated for a voltage jump from −80 to −10 mV; τ_m and τ_h decreased as the step potential was changed from −30 to +20 mV.

5. Outward currents were activated in bathing solutions substantially free of anions and could thus be attributed to potassium ions. The tail current reversed in direction on repolarization to −60 mV when the potassium concentration in the bathing solution was increased from 6 to 30 mM. When the bathing solution contained 145 mM-potassium, and the patch pipette, 95 mM, a depolarization to −10 mV from a holding potential of −60 mV evoked an inward current.

6. Outward currents were examined by using voltage pulses which depolarized the cell to −20 mV, or more positive values, from a holding potential of −80 mV and by pulses which depolarized the cell to 0 mV, or to positive values, from a holding potential of −30 mV. A Boltzmann fit of typical activation data gave a half-maximal activation voltage of 17 mV and a 'slope' of 14 mV.

7. The time course of the rising phase of the current was described by a function of the form $A\{1-\exp[-(t-\delta t)/\tau]\}$, where δt varied between 1 and 4 ms and τ varied between 4 and 27 ms, decreasing with increasing depolarization. There was no evidence for a fast transient component.

MS 8428

8. The amplitude of outward currents was reduced by extracellular calcium ions, cobalt ions, tetraethylammonium and 4-aminopyridine.

9. During prolonged depolarization, the time course of the current could be described by the sum of two exponentially decaying components, with time constants of around 1 and 10 s. 4-Aminopyridine selectively reduced the slower component.

10. Single-channel currents were evoked by depolarization of cell-attached patches with electrodes containing normal extracellular solution. The most frequently encountered channel had a conductance of about 20 pS. Patches usually contained either no or several such channels; the activity of a single channel, however, could be recorded during the inactivation which occurred during prolonged depolarization.

11. A detailed study was made of records obtained from one cell in response to two different voltage jumps. With the 46 mV jump, bursts of openings of 26 ms average duration occurred, separated by interburst periods of 74 ms average duration; the 'open probability' was 0·26. With the 82 mV jump, bursts could not be distinguished; the open probability was 0·90.

12. If events shorter than 1 ms were disregarded, the probability density functions for open times were single exponentials with time constants of 8·5 ms for the 46 mV jump and 18 ms for the 82 mV jump. Two exponential components were required to describe the probability density function for the closed times with time constants of 1 and 70 ms for the 46 mV jump, and 1 and 10 ms for the 82 mV jump.

13. On the basis of these probability density functions, the whole-cell outward currents would be expected to be about six times larger for a voltage jump of 82 mV than for one of 46 mV and to rise at about twice the rate. This is consistent with what was observed.

INTRODUCTION

The human neuroblastoma cell line IMR-32 (Tumilowicz, Nichols, Cholen & Greene, 1970) has been the subject of various biochemical, pharmacological and differentiation studies (see e.g. Gupta, Notter, Felten & Gash, 1985; Clementi, Cabrini, Gotti & Sher, 1986; Sher, Gotti, Pandiella, Madeddu & Clementi, 1988). However, little is known of the electrical properties of these cells. Voltage-dependent inward and outward currents have been reported by Gotti, Sher, Cabrini, Bondiolotti, Wanke, Mancinella & Clementi (1987) and by Ginsborg, Martin & Patmore, (1987); Sher *et al.* (1988) have also demonstrated that calcium entry may be stimulated by depolarization, and Carbone, Sher & Clementi (1990) have given a detailed description of voltage-activated calcium currents. However, the sodium and potassium currents do not appear to have been investigated in detail, and the purpose of this paper is to provide a fuller account. We show that the undifferentiated IMR-32 cell can fire an action potential and can generate classical sodium and delayed-rectifier potassium currents (see e.g. Hille, 1984); the latter reflects the existence of voltage-sensitive channels of about 20 pS conductance.

METHODS

The experiments were done on about 120 cells between August 1985 and October 1987.

Cell cultures

The IMR-32 cell line was obtained from Flow laboratories and grown in 75 cm^2 culture flasks containing minimal essential medium (MEM) with Hanks salts and 25 mM-HEPES, 10% fetal calf serum, 100 i.u./ml penicillin and 100 μg/ml streptomycin at pH 7·35. Cells were grown at 37 °C until confluent and then transferred at a low density to 35 mm Petri dishes. No steps were taken

TABLE 1. Composition of solutions (mM)

	A	B	C	D	E	F
NaCl	145	145	6	121	—	10
KCl	6	6	145	30	6	110
$CaCl_2$	2	—	2	2	—	2·5
$MgCl_2$	1	1	1	1	1	1
EGTA	—	—	—	—	—	11
HEPES	10	10	10	10	10	10
Glucose	5	5	5	5	5	—
Sucrose	—	—	—	—	266	—
TTX	0·5 μM	0·5 μM	0·5 μM	0·5 μM	—	—

Solutions A–E were adjusted to pH 7·4 with NaOH. Solution F was adjusted to pH 7·2 with KOH. In some experiments $CoCl_2$ was added to the extracellular solution, as noted in the text. The free calcium concentration in the pipette solution F (whole-cell mode) was estimated as 0·1 μM, taking the value of 6·45 for $pK_{apparent}$ of Ca-EGTA at the ionic strength of the solution (Miller & Smith, 1984; D. J. Miller, personal communication).

EGTA, ethyleneglycol-bis-(β-aminoethylether)*N,N'*-tetracetic acid; HEPES, *N*-2-hydroxyethyl-piperazine-*N'*-2-ethanesulphonic acid; TTX, tetrodotoxin.

to induce morphological differentiation and such processes as were observed were less than 50 μm in length; the cells may therefore be regard as undifferentiated (cf. Gupta *et al.* 1985, who characterized differentiated cells as possessing neurites from 1·4 to 11 mm in length).

Solutions

The compositions of the extracellular solutions are listed in Table 1. In some experiments solution B was modified (B') by the replacement of sodium by tetramethylammonium. For current-clamp recordings the pipettes were filled with solution (G) containing (mM): KCl, 100; $MgCl_2$, 1; $CaCl_2$, 1; EGTA, 11; HEPES, 10; pH adjusted to 7·2 with NaOH. The concentration of ionized calcium was calculated to be 3×10^{-8} M according to the routine kindly provided by Dr D. J. Miller (see Miller & Smith, 1984). For the recording of sodium currents under voltage clamp, potassium was replaced by caesium (140 mM), but the solution (H) was otherwise unchanged.

Drugs

Tetrodotoxin (TTX), tetraethylammonium chloride (TEA) and 4-aminopyridine (4-AP) were obtained from Sigma, dissolved in distilled water and diluted in the appropriate solution.

Electrical recordings

For electrical recordings the dishes containing the cells, bathed in a solution appropriate to the experiment to be done, as detailed below, were mounted on the stage of an inverted microscope. Currents and voltages were recorded by the whole-cell variation of the patch-clamp technique (Hamill, Marty, Neher, Sakmann & Sigworth, 1981) at room temperature (18–22 °C). The patch pipettes were pulled from Corning No. 7052 glass (1·55 mm o.d., 1·0 mm i.d.) and were fire-polished. The pipette resistances in free solution were between 1 and 3 MΩ. If the series resistance is taken as twice that in free solution (Marty & Neher, 1985) the voltage at the tip of the pipette

would differ from the command value by less than 6 mV for currents of up to 1 nA. Since currents in the present experiments were always smaller than 1 nA, resistance compensation was not employed. The values of voltages given in Results are uncorrected command values.

The patch pipette was tightly sealed onto the surface of the cell and the cell broken into by suction. The seal resistance before breaking into the cell was in the range 5–15 GΩ. After the cell was broken into, the input resistance, measured in a series of twelve cells (with 100 mM-K^+ in the pipette, solution G) was $1{\cdot}6 \pm 0{\cdot}7$ GΩ (mean ± S.D.) with a range of 0·8–3·0 GΩ. The EPC-7 amplifier (List electronics, Darmstadt, Germany), was used in the current-clamp mode (with the 1 GΩ feedback resistor), for recording resting membrane potentials and to allow constant-current pulses to be applied to the cell. It was used in the voltage-clamp mode to record voltage-activated currents. Voltage pulses were generated by a CED 1401 interface (Cambridge Electronic Design, Cambridge) under the control of an Apple II microcomputer. Cell capacitance, input resistance and the series resistance were determined from the current response to a 5 mV voltage-clamp pulse.

Data analysis

Electrical signals were recorded on magnetic tape with an FM tape-recorder (Racal Store 4D). Analog-to-digital and digital-to-analog conversions were performed at 12-bit resolution by means of the microcomputer and interface. Digitized records were stored on floppy disc for subsequent analysis. Sodium currents were usually recorded at 30 in/s and were replayed at 7·5 in/s, filtered with an 8-pole Bessel filter (−3 dB at 4 kHz) and digitized at 40 kHz; this is equivalent to 160 kHz sampling of the original recordings so that 6·4 ms of the original signal contained 1024 points. Correction for capacitance and leakage were made as described in Results and the corrected digital data transferred to the D–A converter of the CED 1401 interface (together with a suitable ramp to provide the time base) and thence to an analog plotter. Whole-cell outward currents were usually recorded at 7·5 in/s and, for analysis, replayed at the same speed, filtered with an 8-pole Bessel filter(−3 dB at 0·1 to 0·25 kHz) and digitized at 1–2·5 kHz. 'Hard copy' was produced either in the same way as described above for sodium current records or by sending the digital data to a digital plotter via the Easygraph programme provided by Edinburgh University Computing Service (EUCS) on its mainframe computer. Curves were fitted to the data by non-linear regression with the help of NAG (Numerical Algorithms Group, Oxford) minimizing routines E04JAF or E04CCF, also made available by EUCS.

Cell-attached patches

Standard techniques were used to obtain cell-attached patches (Hamill *et al.* 1981). Single-channel current records were made with the List EPC-7 amplifier (10 GΩ feedback resistor; List, Darmstadt, Germany) and recorded on magnetic tape at 7·5 ins/s (Racal Store 4). Channels were activated by depolarizing pulses; in general, responses to hyperpolarizing pulses consisted only of the capacitative and linear leakage components, and could therefore be used to correct the responses to depolarization in the same way as for whole-cell responses.

Data processing: preliminary test of stationarity

The tape was played back into the CED 1401 interface connected to a DCS 286 microcomputer under the control of PAT software (kindly provided by J. Dempster, Department of Physiology and Pharmacology, University of Strathclyde). Records were filtered with an 8-pole Bessel filter, −3 dB at 1 kHz and sampled at intervals of 100 μs. The PAT software produced files of open and closed durations which were inspected using the cusum technique (see Glasbey & Martin, 1986) to allow sections to be selected for stationarity. The cusum, S_j, for open times, say, is given by

$$S_j = \Sigma(X_i - X_m), \quad i = 1 \text{ to } j, \quad \text{for } j = 1, \ldots . n, \tag{1}$$

where X_i is the rank order of the duration of the ith open period and X_m (which equals $n(n+1)/2$) is the mean rank. A random fluctuation about zero is expected for channels which show stationary behaviour. The significance of the deviation may be estimated by determining a test statistic, D_α, the maximum value of

$$|S_j|/\{1 + (\alpha - 1)j/n\}, \tag{2}$$

for $j = 1$ to n, and calculating

$$2\exp(-12\alpha D_\alpha^2/nX_m), \tag{3}$$

which is the approximate probability of obtaining a value larger than D_α for a sequence of random events. This test was applied for values of $\alpha = 9, 1, 1/9$ and the procedure was also applied to the closed times.

Probability density functions (PDFs)

PDFs for open and closed states were obtained from the selected single-channel data by the method of maximum likelihood (see Colquhoun & Sigworth, 1983), with the help of the NAG minimizing subroutine, E04CCF. The fitting procedure requires the selection of the minimum interval, t_m, that can be reliably observed. When this was set to a value below 0·9 ms, it was found that the open times were best fitted by a two-component PDF (time constants, τ_o' and τ_o, say) and the closed times by a three-component PDF (time constants, τ_f', τ_f and τ_s, say). However, the components with the time constants τ_o' and τ_f', which were smaller than t_m, dominated the PDFs and corresponded to unrealistically large numbers of 'missed' events; moreover, although the values of τ_o, τ_f and τ_s were relatively stable, values for τ_o' and τ_f' varied randomly with the choice of t_m. When t_m was set to 1 ms, the open times could be adequately fitted by a single exponential function with time constant close to τ_o and the closed times by the sum of two exponential functions with time constants close to τ_f and τ_s. Thus the PDFs for the open (4) and closed (5) times may be denoted:

$$(1/\tau_o)\exp(-t/\tau_o), \tag{4}$$

and

$$(a_s/\tau_s)\exp(-t/\tau_s)+(a_f/\tau_f)\exp(-t/\tau_f). \tag{5}$$

where $a_f = 1-a_s$. A rough check of the validity of the PDFs may be obtained by comparing the observed 'equilibrium' open probability, $p_{1\infty}$, say, i.e. the mean open time/(mean open time + mean closed time), with that predicted on the basis of the PDFs evidently given by

$$p_{1\infty} = \tau_o/(\tau_o+a_s\tau_s+a_f\tau_f). \tag{6}$$

As already shown by Sakmann & Trube (1984) in a somewhat different way, the predicted value of $p_{1\infty}$ depends on the PDFs of the open and closed times and is independent of the underlying kinetic model. The relative amplitudes and the time courses of the rising phases of the whole-cell currents that would be predicted on the basis of the PDFs were calculated as sketched below (cf. Sakmann & Trube, 1984, who cover some of the same ground; it may be noted that their eqn (24), p. 679, is defective).

The general form predicted from the PDFs for the time course of the open probability, $p_1(t)$, say, during the response to a voltage jump is given by

$$p_1(t) = p_{1\infty}-A\exp(-t/\tau_1)-B\exp(-t/\tau_2), \tag{7}$$

(see Colquhoun & Hawkes, 1977, 1981, 1982). A and B depend upon the initial conditions and the particular kinetic model, but τ_1 and τ_2 depend only on the PDFs. They are such that

$$\tau_1+\tau_2 = (\tau_o\tau_s+\tau_s\tau_f+\tau_f\tau_o)/(\tau_o+a_s\tau_s+a_f\tau_f) \tag{8}$$

and

$$\tau_1\tau_2 = \tau_o\tau_s\tau_f/(\tau_o+a_s\tau_s+a_f\tau_f). \tag{9}$$

For the kinetic model, $C_2 \rightleftharpoons C_1 \rightleftharpoons O$, if p_{10} and p_{20} denote the probability of states O and C_1, respectively at $t = 0$,

$$A = \{\tau_1 p_{1\infty}-p_{10}\tau_1(1-\tau_2/\tau_o)-p_{20}(a_f\tau_s+a_s\tau_f)p_{1\infty}\}/\{\tau_1-\tau_2\}, \tag{10}$$

and

$$B = p_{1\infty}-A. \tag{11}$$

If it is assumed that at $t = 0$, all the channels are in state C_2 then $p_{10} = p_{20} = 0$, and the time course shown in eqn (4) simplifies to

$$p_1(t) = p_{1\infty}[1-\{\tau_1\exp(-t/\tau_1)-\tau_2\exp(-t/\tau_2)\}/\{\tau_1-\tau_2\}]. \tag{12}$$

For the kinetic model $C_2 \rightleftharpoons O \rightleftharpoons C_1$, the expressions corresponding to eqns (10), (11) and (12) are:

$$A' = \{(\tau_1-\tau_f)p_{1\infty}-p_{10}\tau_2(\tau_1/\tau_f-1)-p_{20}(\tau_s-\tau_f)p_{1\infty}\}/\{\tau_1-\tau_2\}, \tag{13}$$

$$B' = p_{1\infty}-A' \tag{14}$$

$$p_1'(t) = p_{1\infty}[1-\{(\tau_1-\tau_f)\exp(-t/\tau_1)+(\tau_2-\tau_f)\exp(-t/\tau_2)\}/\{\tau_1-\tau_f\}]. \tag{15}$$

During the 46 mV depolarizations, it was possible to distinguish separate bursts of channel activation. The mean duration, t_b, of bursts predicted from the PDFs shown in eqns (4) and (5) are formally different for the two kinetic models. From the results of Colquhoun & Hawkes (1982) it may be shown that for the CCO model,

$$t_b = (1+\Phi^2 a_f/a_s)/\tau_o + \Phi^2 a_f \tau_s \tau_f / \{a_s(a_s+\Phi^2 a_f)(\tau_s-\tau_f)\}, \quad (16)$$

where $\Phi = 1+\tau_f/\{a_f(\tau_s-\tau_f)\}$.

For the COC model,

$$t'_b = (\tau_o + a_f\tau_f)/a_s. \quad (17)$$

When τ_s is much greater than τ_f, which will be the case if bursts can be distinguished, Φ tends to 1 and eqn (16) reduces to eqn (17).

RESULTS

Resting and action potentials recorded under current clamp

In a series of fifty-two cells, where the patch pipette contained a high concentration of potassium (solution G, Methods), the resting potential had a mean of -38 ± 11 mV (mean $\pm$ S.D.) and ranged between -17 and -72 mV. The resting potentials of the majority of the cells (40) were between -30 and -60 mV; this range is similar to that reported for the mouse neuroblastoma, N1E-115 (-35 to -55 mV) by Moolenaar & Spector (1978). The values for IMR-32 cells are likely to be underestimates since the seal resistance was not often more than 5 times the cell input resistance, which could be as large as 3 GΩ (see Methods). Figure 1 illustrates an experiment in which the potential of a cell was hyperpolarized from its resting value of -42 mV to about -80 mV by passing an inward current of 30 pA (not shown) under current clamp. Responses were then observed to superimposed hyperpolarizing and depolarizing pulses of different amplitudes. Over the range of small current pulses (e.g. Fig. 1*a* and *b*) the voltage–current relation was linear, its slope corresponding to an input resistance of about 1·3 GΩ. With increasing depolarizations, the electrotonic potentials gave rise to local responses (e.g. Fig. 1*c*), and, at a threshold of between -45 and -35 mV, to an action potential (e.g. Fig. 1*d* and *e*) which was followed by a small undershoot. Only a single action potential occurred no matter how long or larger the current pulse, although on occasions the action potential was followed by a series of oscillations. The magnitude of the action potential increased with increasing stimulating current. In Fig. 1*d* the current was 75 pA and the action potential was 83 mV; in Fig. 1*e* the current was increased to 100 pA and the action potential amplitude rose to 92 mV. This corresponds to an input resistance of 0·36 GΩ at the peak of the action potential (as compared to the value 1·3 GΩ at -80 mV, mentioned above).

Voltage clamp

Sodium currents

As reported by Gotti *et al.* (1987), when the cell was under voltage clamp and the pipette contained a high concentration of potassium (solution G, Methods), the response to depolarization from a sufficiently negative holding potential consisted of a rapid inward followed by a sustained outward current. The sustained outward component was not seen if the potassium in the pipette was replaced with caesium (solution H, Methods); it could therefore be identified as a potassium current. The

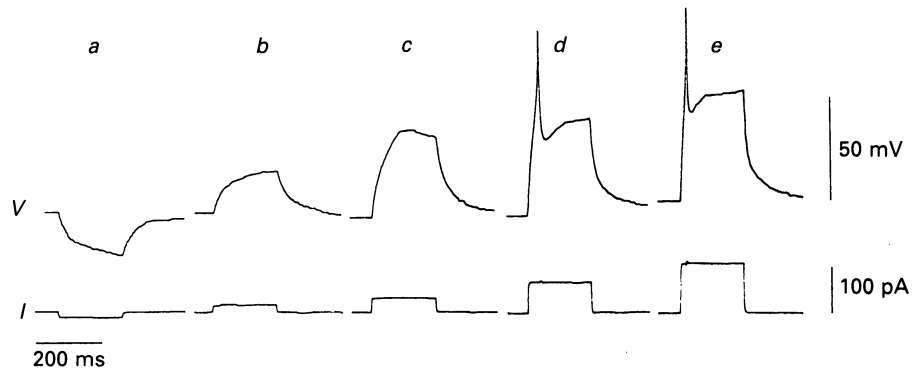

Fig. 1. Voltage responses (V) of IMR-32 cell to constant-current pulses (I). Resting potential, −42 mV; a steady inward current of about 30 pA was passed to set membrane potential to about −80 mV before applying current pulses. The extracellular solution (Table 1, solution A) contained 145 mM-Na^+ and pipette (solution G, Methods), 100 mM-K^+.

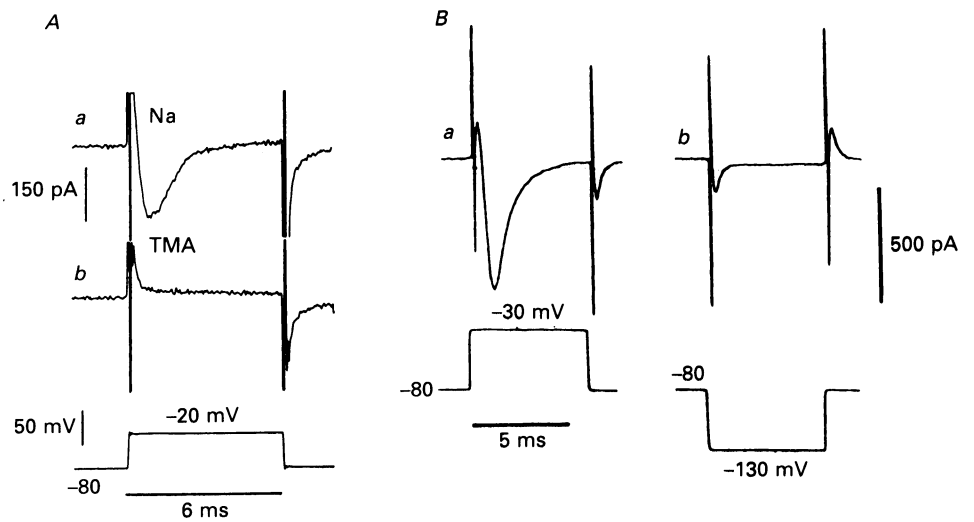

Fig. 2. Current responses of two different IMR-32 cells (A and B) to voltage steps applied under voltage clamp. Signals were recorded on magnetic tape at 60 in/s and replayed at $1\frac{7}{8}$ in/s into a pen recorder. The pipette contained 140 mM-CsCl (solution H, methods). A, effect of replacement of Na^+ by TMA^+; cell held at −80 mV and stepped to −20 mV for 6 ms. Aa, response in 145 mM-Na^+ (Table 1, solution A); Ab, abolition of transient inward current when Na^+ was replaced with 145 mM-TMA^+ (solution B′, Methods). B, comparison of responses to a depolarizing voltage step (a) and a hyperpolarizing voltage step of same amplitude (b) . Holding potential, −80 mV; pulse amplitude, 50 mV. Note that the response to a hyperpolarizing pulse consists only of symmetrical capacitative currents at the beginning and end of the pulse, together with a small steady inward current during the pulse. The extracellular solution (Table 1, solution B) contained 145 mM-Na^+ and no added Ca^{2+}.

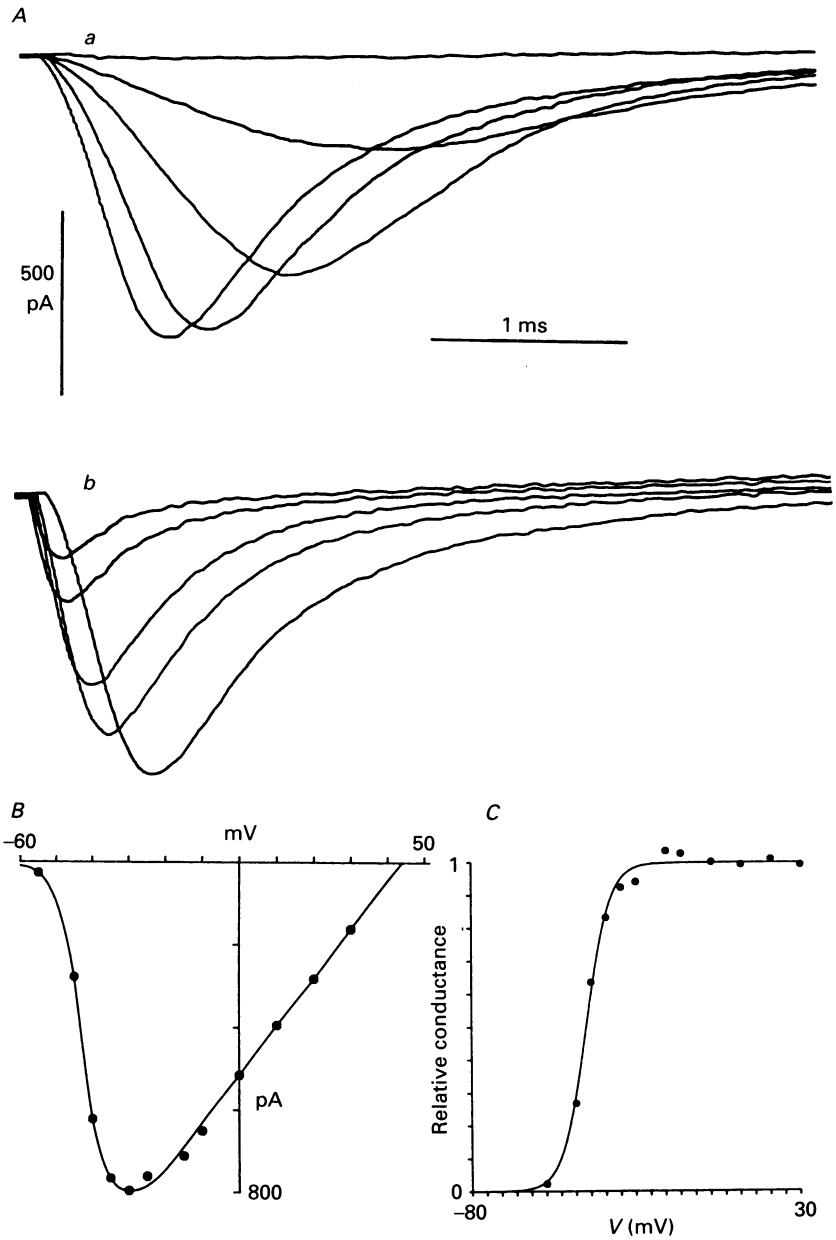

Fig. 3. Activation of inward current in a single IMR-32 cell by depolarizations of different amplitudes from a constant holding potential of −80 mV. The pipette contained 140 mM-CsCl (solution H, Methods); the extracellular solution (Table 1, solution A) contained 145 mM-Na^+. Individual responses were digitized and corrected for linear leakage and capacitative currents by proportional addition of the current evoked by a 25 mV hyperpolarizing pulse (cf. Fig. 2*B*). Records shown are averages of four to six individually corrected responses for each voltage step (not shown). The current transient during the rising phase of the voltage step has been blanked out and it should be noted that the initial 300 μs of record may not be reliable because of its critical dependence on the accuracy of correction. In *Aa*, responses are shown, in order of increasing amplitude, to depolarizing voltage steps of 25, 30, 40, 45 and 50 mV; in *Ab*, responses are shown, in

inward component could be suppressed by removal of sodium ions from the bathing solution or by the addition of 0·5 μM-TTX and could therefore be identified as a sodium current. Figure 2*Aa* shows an individual uncorrected pen record of the response of a cell held at −80 mV, and bathed in a sodium-containing solution (Table 1, solution *A*), to a 60 mV depolarizing pulse. The effect of replacement of the extracellular sodium with tetramethylammonium (solution B′, Methods) which clearly abolished the inward current, is shown in Fig. 2*Ab*.

Sodium currents were seen in over half the cells in which they were sought. Thus in a series of seventeen cells, thirteen showed active inward currents similar to those described here. The peak amplitudes ranged from 50 to 960 pA when the cell was held between −70 and −80 mV and depolarized by 60 mV; the amplitudes were not related to the size of the cell or to any other identifiable property.

Figure 2*Ba* shows another example of an uncorrected Na^+ current from a different cell, held at −80 mV and depolarized by 50 mV. Figure 2 *Bb* shows the effect of an equal hyperpolarization: the response evidently consists of approximately symmetrical capacitative currents at the beginning and end of the pulse and a small steady inward current during the pulse. The amplitude of such responses varied linearly with the amplitude of the hyperpolarizing voltage pulse and thus could be used to correct the sodium current records by proportional addition.

Activation of sodium current. A family of sodium currents evoked by increasing depolarizing steps from a holding potential of −80 mV and corrected for leakage and capacitative artifacts is shown in Fig. 3*A*. As can be seen in *Aa* the currents increased in peak amplitude with depolarization up to a value of about −25 mV and thereafter, as seen in *Ab*, decreased with a further increase in depolarization; the time to the peak of the current decreased monotonically with increasing depolarization. All the data from this cell relating peak current to voltage are shown in Fig. 3*B*. The maximum current was 800 pA and the extrapolated reversal potential was +44 mV.

The activation characteristics of the sodium currents shown in Fig. 3*A* were analysed by estimating the conductance (g) at different depolarizations according to the relation $I = g(V - E_{Na})$, where I refers to peak current values; this assumes that the instantaneous current–voltage relation is linear. The data were then fitted to the Boltzmann equation:

$$g = g_{max}/\{1 + \exp[(V - V_h)/k]\}, \quad (18)$$

where g is the conductance, g_{max}, the maximum conductance, V, the test potential, V_h, the 'half-activation' potential and k defines the slope. The peak conductance was 11·7 nS; as illustrated in Fig. 3*C*, V_h was 41·6 mV and k was 3·9 mV.

Steady-state inactivation. Inactivation of the sodium current was investigated by altering the holding potential and stepping the membrane potential to −20 mV (Fig. 4). A depolarization of the holding potential of the cell from −120 to −65 mV caused a progressive decrease in the amplitude of the inward current without any obvious

order of decreasing amplitude, to voltage steps of 55, 70, 80, 100 and 110 mV. *B* shows the relation between peak current and voltage derived from all the data for this cell. Curve drawn by eye: voltages were not corrected for the effect of pipette resistance (see Methods) and the maximum inward current may thus have occurred at a slightly more positive voltage (by up to 5 mV) than shown. *C*, 'Boltzmann' fit of the conductance–voltage relation (see text).

change in its time course. The normalized currents evoked from different holding potentials were plotted against those potentials (Fig. 4*B*). The data were fitted (cf. eqn. (18)) to:

$$I = I_{max}/\{1+\exp[(V_h - V)/k]\}, \quad (19)$$

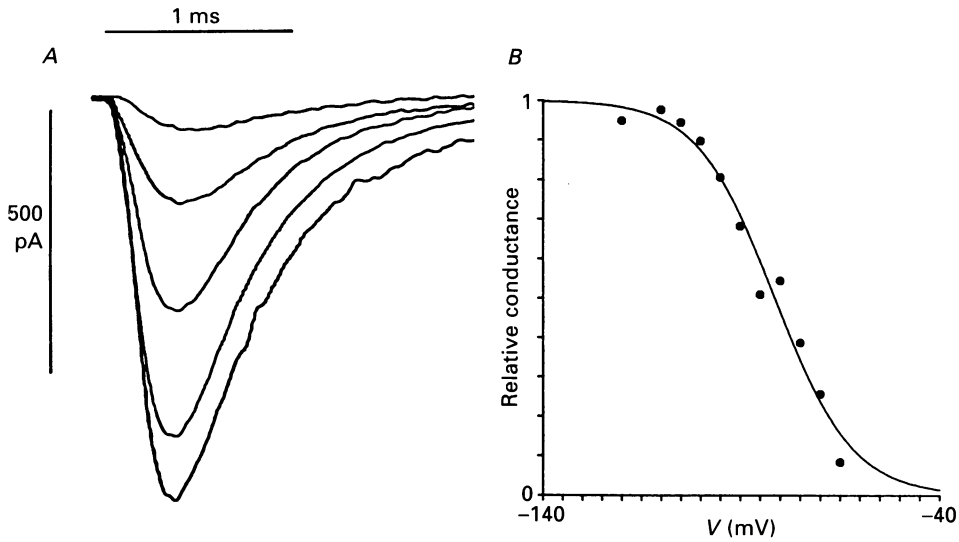

Fig. 4. Inactivation of sodium current at different holding potentials. Solutions as in experiment of Fig. 3. The cell was depolarized to −20 mV from various different holding potentials. In *A*, each record is the average of four to six individual responses corrected as described in the legend to Fig. 3. The holding potentials in order of increasing amplitude of responses were −65, −70, −85, −95 and −120 mV. *B*, Boltzmann fit of all the data from this experiment.

where I is the current, I_{max} is the maximum current, V_h is the voltage at which the current is half-inactivated, V is the membrane potential and k defines the slope. V_h was −81 mV and k was 9·7 mV. At the observed resting potentials of these cells the sodium current would be almost completely inactivated.

Time dependence of activation and inactivation of I_{Na}. In an attempt to see how far the observed sodium current was consistent with the classical model of Hodgkin & Huxley (1952) the time course of the currents evoked by various voltage jumps from −80 mV was compared with that given by the simplified equation:

$$I_{Na} = I\{1-\exp(-t/\tau_m)\}^3\exp(-t/\tau_h), \quad (20)$$

where τ_m and τ_h were estimated from the falling phase of the observed current by non-linear least-squares regression. The fitted values of τ_m and τ_h for the different currents analysed are shown in Fig. 5*B*. As pointed out by Belluzzi & Sacchi (1986), the time to peak predicted by eqn (20) is $\tau_m \ln(1+3\tau_h/\tau_m)$. A comparison of the predicted and observed values for the experiments illustrated in Fig. 3 is shown in Table 2. The observed times to peak decrease in much the same way as predicted, although the absolute values are 200–300 μs larger.

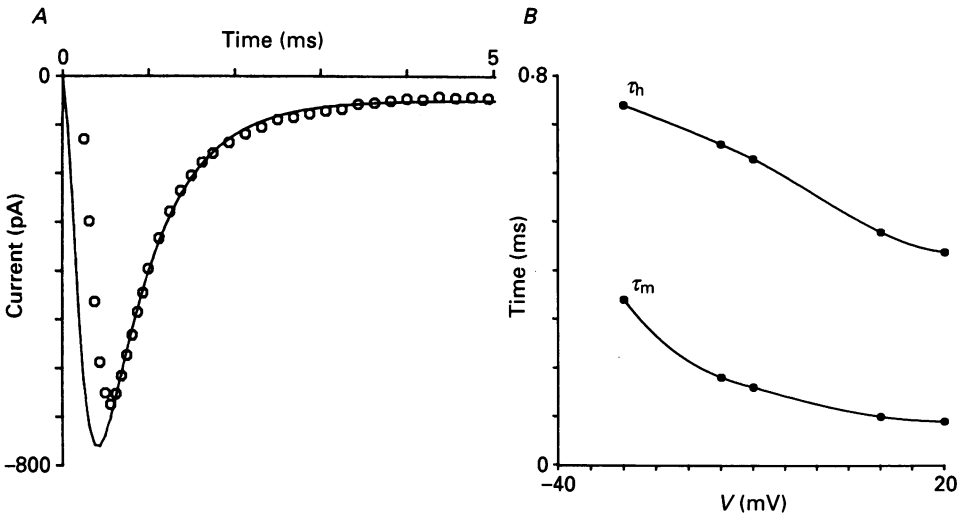

Fig. 5. Analysis of time course of sodium current. *A*, continuous curve shows the best fit of the form

$$I_{Na} = I\{1-\exp(-t/\tau_m)\}^3 \exp(-t/\tau_h),$$

to the falling phase (from 0·5 ms after start of the record) of the response to a voltage jump from −80 to −20 mV. ○, observed current. *B*, values of τ_m and τ_h estimated from best fits, as in *A*, to responses evoked by jumps from −80 mV to the different voltages. Curves drawn by eye.

TABLE 2. Comparison of observed and calculated times to peak sodium current

	Voltage (mV)				
	−30	−15	−10	10	20
Calculated time to peak (ms)	0·7	0·57	0·41	0·27	0·24
Observed time to peak (ms)	0·98	0·72	0·64	0·49	0·44

The model provided a good fit to the declining phase of the current. The rising phase is less well described but this is not surprising since its time course is critically dependent on the accuracy of the correction for capacitative current.

Potassium currents

In most experiments, outward currents were corrected by algebraic addition of a number of smaller currents evoked by appropriate hyperpolarizing pulses (Bezanilla & Armstrong, 1977). It was sometimes possible to correct by adding currents evoked by equal (but opposite) voltage jumps. This is illustrated in Fig. 6*A* from an experiment in which a cell was held at −60 mV, depolarized by 60 mV (*a*), and hyperpolarized by 60 mV (*b*). In *Ac*, the currents are superimposed to eliminate the capacitative artifact and the leakage current (including the passive linear current component). *Ad* shows the average of four such superimpositions. The initial inward deflection (1) shows the presence of a small sodium current which was absent when tetrodotoxin was added to the extracellular solution; '2' indicates the presence of a small outward tail-current.

In some experiments the capacitative artifact and the leakage currents were sufficiently small to make corrections unnecessary, and data processing was confined to averaging a number of uncorrected responses to depolarizing pulses. An example is shown in Fig. 6*B* in which sixteen responses were evoked at intervals of 10 s; the

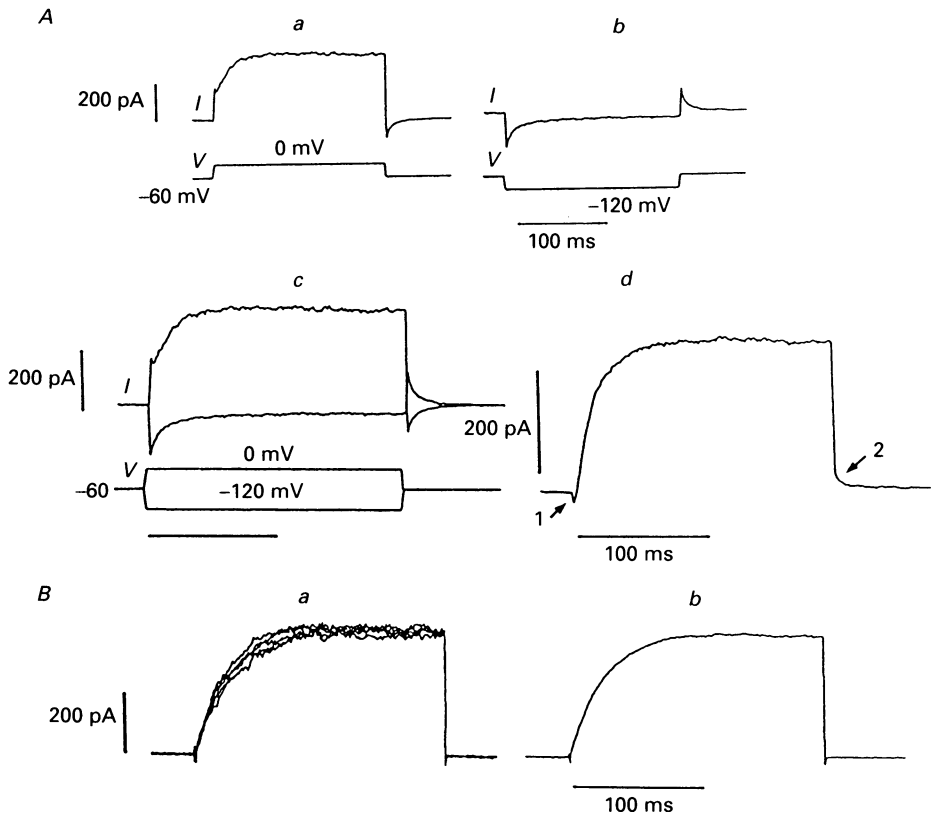

Fig. 6. Outward currents evoked by depolarization of IMR-32 cells. *A*, cell held at −60 mV depolarized to 0 mV (*a*) or hyperpolarized to −120 mV (*b*) during 200 ms voltage jumps. *I*, current (upward deflections in this and all other records correspond to outward currents); *V*, voltage (depolarization upward). In *Ac*, *a* and *b* are superimposed; *Ad* shows the average of the sum of four such pairs. The initial inward deflection (1) is presumably a sodium current; note the outward tail current (2). The resting potential of the cell was −62 mV. Extracellular solution as in Table 1, solution B, but without tetrodotoxin. *B*, cell held at −80 mV; currents evoked by 200 ms voltage jumps of 90 mV. *Ba*, individual, randomly fluctuating, responses; *Bb* shows the average of sixteen such responses. Voltage jumps applied at 10 s intervals. Extracellular solution as in Table 1, solution B.

five superimposed traces (responses to stimuli 1, 3, 5, 7 and 10) in Fig. 6*Ba* illustrate the random fluctuations in current which occur from stimulus to stimulus. The average of the set of sixteen responses is shown in Fig. 6*Bb*. In this experiment there was evidently no 'run-down', but it should be noted that stable current responses were not always obtained, even with high resistance seals, and 'run-down' was the usual reason for abandoning a cell.

Current–voltage relationships

In the experiment illustrated in Fig. 7, the extracellular solution contained no added calcium, and the usual NaCl content was replaced by sucrose. Inward cationic currents were thus eliminated, as was also the possibility of an outward current

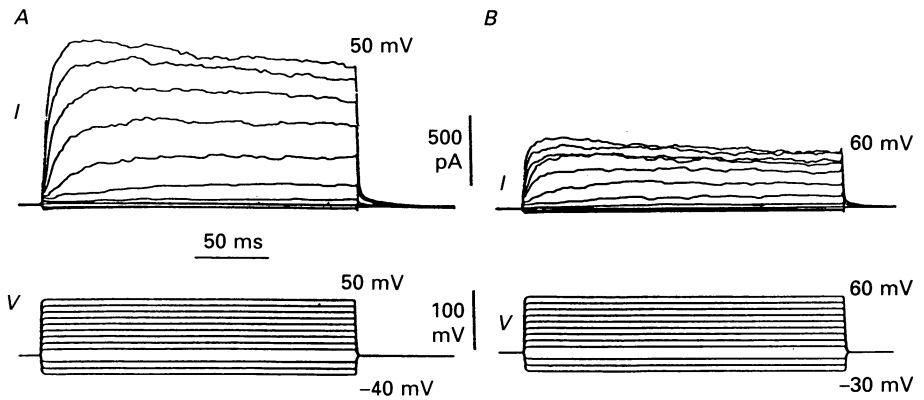

Fig. 7. Uncorrected current responses of cell bathed in low-chloride solution (28 mM; Table 1, solution E, but with 10 mM-$CoCl_2$) recorded with pipette containing high-chloride solution (112 mM; Table 1, solution F). Cell held at −40 mV (*A*) and −30 mV (*B*), hyperpolarized by 30 mV and depolarized by 90 mV in 10 mV steps during 200 ms voltage jumps. *I*, current; *V*, voltage.

carried by an influx of chloride ions. Families of responses to depolarizing and hyperpolarizing voltage steps from a holding potential of −40 mV are shown in *A*, and from a holding potential of −30 mV in *B*. In each set, the lowest current records, which cannot be distinguished from one another, show the responses to hyperpolarizations of 10, 20 and 30 mV. The very small inward currents are consistent with there being little, if any, sustained outward current at the holding potentials of −40 and −30 mV, and therefore little current to be suppressed by hyperpolarization. This was a general result, and there is thus no evidence for an M-current (see e.g. Adams, Brown & Constanti, 1982) in IMR-32 cells. The upper traces demonstrate that relatively large outward currents can be evoked at holding potentials as positive as −40 and −30 mV which inactivate to only a small degree during a 200 ms pulse. The results strongly suggest the presence of a delayed rectifier current, I_K.

Effects of high K^+ on currents

In Fig. 8*Aa*, with an extracellular concentration of potassium on 6 mM, the tail current (*t*, arrow) is outward; in *Ab* with 30 mM-extracellular potassium, the tail current (*t*, arrow) is inward, indicating that the equilibrium potential for the ion(s) carrying the current has changed from a level more negative than −60 mV to one less negative. In *B*, the concentration was raised from 6 mM (in *a*) to 145 mM (in *b*),

a concentration presumably greater than the intracellular value, since the recording electrode contained only about 100 mM-potassium; depolarization from −60 to −10 mV now caused an inward current. On repolarization to −60 mV the inward current increased further because of the increased driving force. From the current

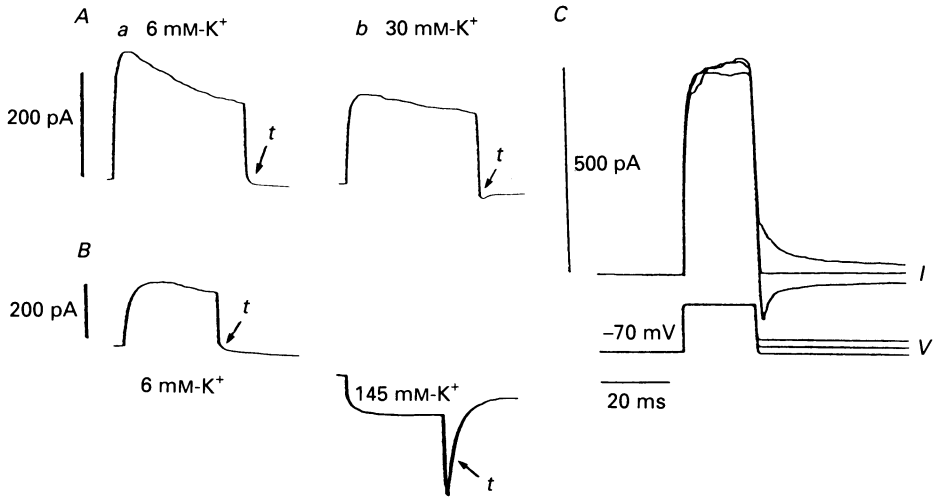

Fig. 8. Effect of an increase in extracellular potassium on currents evoked by depolarization. Records are averages of nineteen responses, corrected as in the experiment of Fig. 6*A*. *A*, cell held at −60 mV and depolarized to 0 mV during 200 ms voltage jump. In *Aa*, the extracellular potassium concentration was 6 mM (Table 1, solution A); in *Ab* it was increased to 30 mM (Table 1, solution D). Note the reversal of the direction of the tail current (arrow, *t*). *B*, cell held at −60 mV and depolarized to −10 mV for 200 ms. In *Ba* the potassium concentration was 6 mM (Table 1, solution A); in *Bb* it was increased to 145 mM (Table 1, solution C). Note the reversal of the current (see text). *C*, reversal potential for outward current in potassium concentration of 6 mM (Table 1, solution A). *I*, current; *V*, voltage. The cell was depolarized from a holding potential of −70 mV to +50 mV and repolarized to −40 mV to give an outward tail current, to −55 mV to give zero tail current and to −70 mV to give an inward tail current.

'jumps' which occurred at the end of the 50 mV voltage 'jumps', it is possible to infer that the depolarization caused a considerably greater increase in conductance, g say, in the higher external potassium. Thus g (at −10 mV) was 3·3 nS in 6 mM-potassium and 5·7 nS in 145 mM-potassium. A similar effect has been noted for I_K in other cells (see e.g. Dubois, 1981*a*; Sah, Gibb & Gage, 1988).

Reversal potential

Although a systematic study of the equilibrium potential for the tail current was not made, a range of values deduced from the direction of the current at different holding potentials may be given: −55 mV (1 cell, Fig. 8*C*), −60 mV (1 cell), −70 mV (1 cell), −80 to −85 mV (3 cells); six other cells had outward tail currents at −60 mV, and hence equilibrium potentials more negative than this value.

Activation of outward current

In the experiment of Fig. 9, the cell was held at −80 mV and depolarized by 10 mV steps from −30 mV up to +60 mV. A selection of corrected records is shown in *A*. The corresponding values of the conductances are plotted in *B* which also shows a

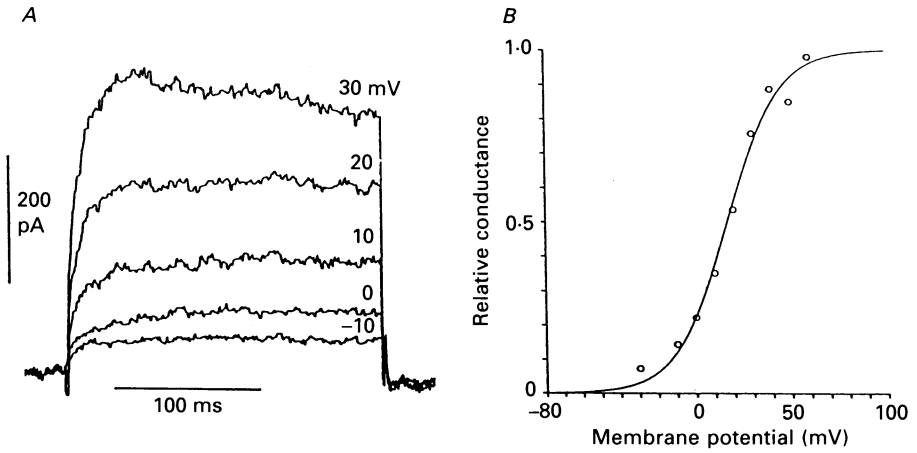

Fig. 9. Current responses of cell bathed in low chloride concentrations (8 mM; Table 1, solution E) recorded with a pipette containing high chloride (112 mM; Table 1, solution F). The cell was held at −80 mV, hyperpolarized to −110 mV and depolarized to +60 mV in steps of 10 mV during 200 ms voltage jumps. *A*, selection of corrected responses to indicated depolarizations. *B*, Boltzmann fit of data shown in *A* on assumptions that the 'instantaneous voltage–current' relation is linear and that the potassium equilibrium potential was −80 mV.

Boltzman curve, $g/g_{max} = 1/(1+\exp\{(V-V_h)/k\})$ where g_{max}, V_h and k were estimated from the data as described earlier. The value of k, 12·9 mV, is similar to that obtained in several other cells (e.g. squid axon, 12 mV, Hodgkin & Huxley, 1952; rat sympathetic neurone, 10 mV, Belluzzi, Sacchi & Wanke, 1985*b*; guinea-pig hippocampal cells, 13·6 mV, Sah *et al.* 1988). Values of 13 and 16 mV were obtained for V_h and of 19 and 13 mV for k in two other experiments which were less satisfactory than that illustrated.

Is there a transient voltage-dependent current, I_A?

As illustrated in Fig. 9, where the holding potential was −80 mV, depolarization did not evoke a rapid transient component of outward current corresponding to I_A which is a prominent feature in many other cells (e.g. Connor & Stevens, 1971; Neher, 1971; Kostyuk, Veselovsky, Fedulova & Tsyndrenko, 1981; Adams *et al.* 1982; Gustafsson, Galvan, Grafe & Wigstrom, 1982; Belluzzi, Sacchi & Wanke, 1985*a*). Although some degree of inactivation often occurred during 200 ms pulses, it did not appear to correspond to the presence of a classical I_A component. First, inactivation occurred even with holding potentials as positive as −40 mV; secondly, with such negative holding potentials as −80 or −90 mV, when an initial peak occurred it was prominent only when the cell was depolarized to 0 mV or beyond and increased with

increasing depolarization. Ypey & Clapham (1984) have described a delayed outward-rectifying potassium conductance with similar properties recorded from cultured mouse peritoneal macrophages. These properties do not correspond to those of classical I_A's, although, as has been pointed out by Rudy (1988), the distinction

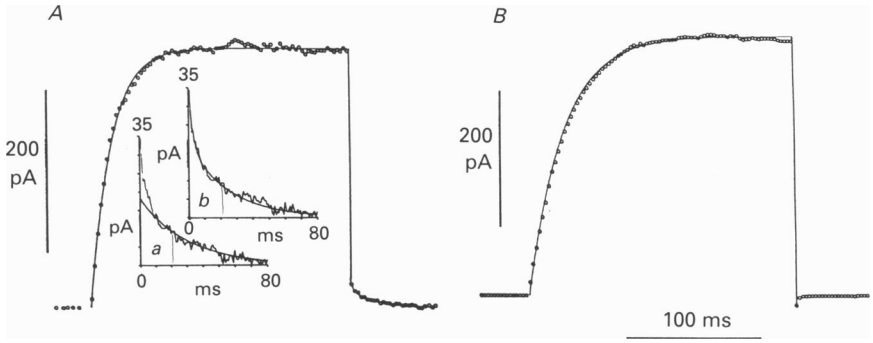

Fig. 10. Analysis of time course of currents shown in Fig. 6. *A* corresponds to Fig. 6*Ad*; holding potential, −60 mV. The line-fitting rising phase is:

$$312\{1-\exp[-(t-3{\cdot}1)/15{\cdot}6]\}.$$

The line fitting tail is:

$$15\exp(-t/2)+22\exp(-t/25).$$

○, experimental values; first point above baseline is at 9·4 ms after start of jump, after which points are at 2·4 ms intervals. Insets show tail current fits at greater resolution: *a* compares data with best single exponential fit, $18\exp(-t/30)$, disregarding first 10 ms of tail; *b* compares data with best double exponential fit as above. *B* corresponds to Fig. 6*Bb*; holding potential, −80 mV. The line-fitting rising phase is:

$$379\{1-\exp[-(t-2{\cdot}4)/26]\}.$$

○, experimental values at 2·4 ms intervals.

between I_A's and I_k's is somewhat blurred, now that a wide range of results is available.

Analysis of time course of currents

In the absence of inactivation, the time course of the rising phase of the outward currents evoked by depolarization could be fitted by the simple empirical relation:

$$I(t) = I_{max}\{1-\exp[-(t-\delta t)/t_1]\}, \quad (21)$$

where δt represents a 'delay' in activation, and t_1 an activation time constant. This relation has been used by Dubois (1981*b*) for the frog node of Ranvier, and provides a convenient way of comparing responses under different conditions. The values of δt were sensitive to the procedure used to correct for the initial capacitative artifact and cannot be regarded as reliable descriptors; the values of t_1 were, however, stable. Figure 10 shows the fitted course of the currents which have already been illustrated in Fig. 6; the particular values for δt and t_1 were 3·1 and 16 ms in *A* and 2·4 and 26 ms in *B*.

Where the current declined during the period of the relatively short depolarizing pulses (up to 300 ms), its time course could be fitted by a simple modification of eqn (21), namely,

$$I(t) = I_1'\{1-\exp[-(t-\delta t'/t_1')]\}\exp[-t/t_i], \quad (22)$$

where t_i may be regarded as a type of 'inactivation' time constant. There was little difference between the values of I_{max} and t_1, derived from fitting eqn (21) to the first 50 ms of the response and I_1' and t_1', derived from eqn (22) fitted throughout the whole time course of the depolarization. The rate of activation increased with increasing

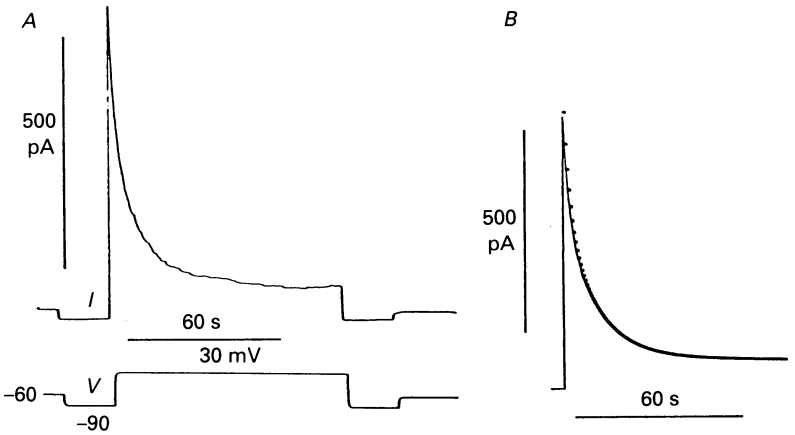

Fig. 11. Inactivation during prolonged depolarization. *A*, current (*I*) produced by 30 mV hyperpolarization followed by 120 mV depolarization (*V*). *B*, outward current compared with double exponential fit (*t* in s):

$$327\exp(-t/1{\cdot}8)+375\exp(-t/9{\cdot}9)+74\ pA.$$

The extracellular solution contained 5 mM- and the pipette 106 mM-potassium.

depolarization: in the experiment of Fig. 9, t_1 fell from 17 ms at 0 mV to 3·6 ms at +60 mV. For six cells which were depolarized to levels between −10 and +10 mV the value of t_1 was 18 ms (range 6–27 ms); for five cells depolarized to between +20 and +60 mV the mean value of t_1 was 8 ms (range 4–15 ms). Values for t_i ranged from about 0·5 to 2 s.

Tail current

The curves in Fig. 10*A* (inset) show fitted time courses of the tail current. As for the frog node of Ranvier (reviewed by Dubois, 1983) and the human T lymphocyte (Cahalan, Chandy, DeCoursey & Gupta, 1985, p. 215), the tail current was best described by the sum of two exponentially decaying components. A similar result was obtained in two other experiments.

Inactivation during prolonged depolarization

The inactivation of the outward current during prolonged depolarization was investigated in a series of experiments, illustrated in Fig. 11, in which a cell was first hyperpolarized to −90 mV, to remove inactivation, and then depolarized to different levels for a period of 90 s. The decline of the current could be fitted by the sum of two exponentially decaying components:

$$I(t) = a_f\exp(-t/t_f)+a_s\exp(-t/t_s), \tag{23}$$

with t_f around 1–2 s and t_s around 10 s; similar results were obtained from two other

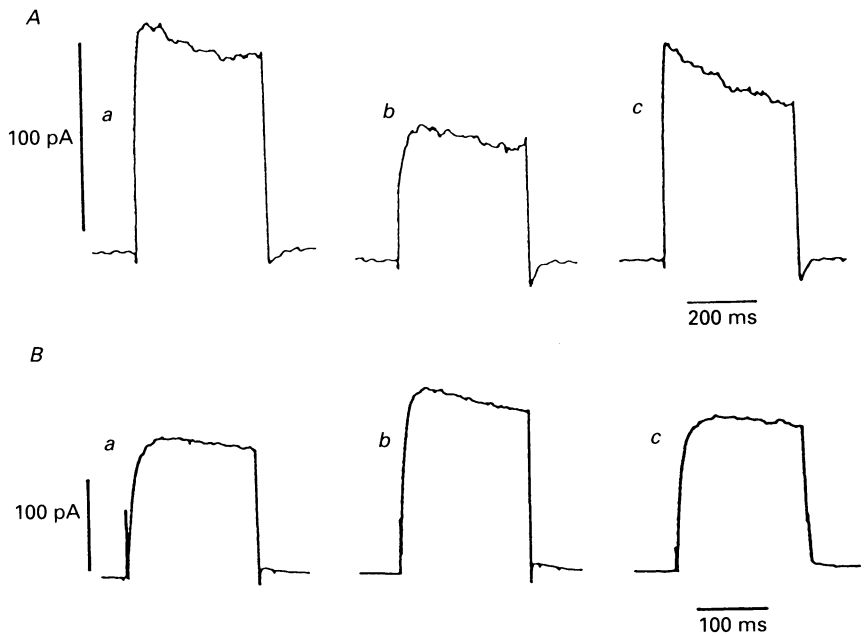

Fig. 12. Effect of calcium on currents. *A*, control responses (*a* and *c*) in 'calcium-free' solution (Table 1, solution B) and test response (*b*) in 2 mM-calcium (Table 1, solution A). *B*, a different cell, control responses (*a* and *c*) in 5 mM-calcium and test response (*b*) in 'calcium-free' solution. Both cells were held at −80 mV and depolarized to 0 mV.

TABLE 3. Inactivation of I_K during prolonged depolarization

Voltage jump	a_f(pA)	t_f(s)	a_s(pA)	t_s(s)
	Cell A			
−90 to −30	214	2·3	65	8·3
−90 to −10	227	1·6	171	7·1
−90 to 0	310	2·3	158	10
−90 to 30	327	1·8	375	9·9
	Cell B			
−60 to 30	423	1·7	236	10
	Cell C			
−60 to 30	485	1·5	325	7·9

cells. These values are within the range for inactivation time constants of delayed rectifier currents in other cells (see e.g. Rudy, 1988). Presumably the time constant, t_f, corresponds to the inactivation time constant, t_i, in eqn (22). Values for the amplitudes and time constants for three cells are shown in Table 3.

Effect of divalent cations

The possible existence of calcium-activated potassium currents was investigated by examining the effects of either adding or withdrawing calcium from the extracellular solution. As illustrated in Fig. 12, the presence of calcium reduced rather than enhanced the outward current. The inhibitory action of calcium was

shared by cobalt. Currents were reduced to between about 0·9 and 0·6 of their control values, in four experiments in which the calcium concentration was either 2 or 5 mM and three experiments with 4 mM-cobalt.

Actions of tetraethylammonium (TEA) and 4-aminopyridine (4-AP)

Although both TEA and 4-AP are known to block a variety of potassium channels, TEA is usually classified as a specific blocker of delayed rectifier potassium currents,

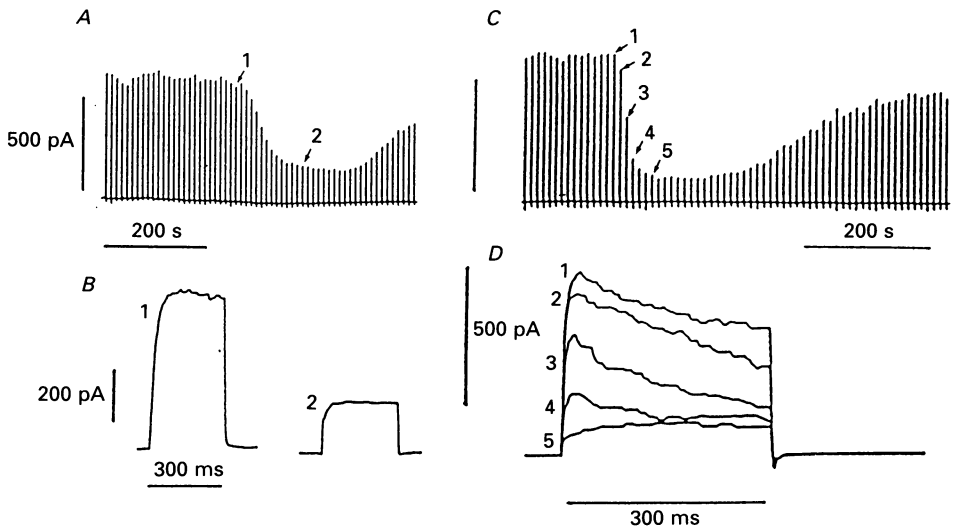

Fig. 13. Effects of TEA and 4-AP. *A*, TEA: responses, recorded on chart recorder, to 300 ms depolarization of 90 mV from holding potential of −70 mV followed by a hyperpolarization of 20 mV. TEA (10 mM) was added to perfusate (Table 1, solution A) at the beginning of record, and removed when outward current was reduced to its minimal value. *B*, individual outward currents at higher resolution, numbered as in *A*. Uncorrected records. *C*, 4-AP: responses, recorded on chart recorder, to 300 ms depolarization of 70 mV from holding potential of −60 mV, followed by an equal hyperpolarization. 4-AP (2 mM) was added to perfusate (Table 1, solution A) at the beginning of record, and removed when the outward current was reduced to its minimal value. *D*, individual outward currents at higher resolution, numbered as in *C*. Uncorrected records.

and 4-AP as a specific blocker of I_A's (see e.g. Cook, 1988). However, 4-AP has been found to block delayed rectifier currents in human T lymphocytes (DeCoursey, Chandy, Gupta & Cahalan, 1984), in mouse Schwann cells (Konishi, 1989) and in chick calcitonin cells (Kawa, 1988).

Both TEA and 4-AP were found to block the outward current in IMR-32 cells as illustrated in Fig. 13. The cells were successively depolarized, and 300 ms later, hyperpolarized, the sequence being repeated at intervals of 10 s. No effect was observed on the inward currents (which can just be seen as small deflections below the baseline with the low amplification used in Fig. 13) but the outward current was rapidly reduced by the addition of TEA to or 4-AP. Concentrations of TEA between

0·5 and 20 mM were investigated in six experiments. No effect was observed with 1 mM-TEA or less, but the results were not otherwise sufficiently consistent for quantitative analysis.

The action of 4-AP was examined in greater detail, as illustrated in Fig. 14. As first reported for the delayed rectifier current of the squid axon by Yeh, Oxford, Wu &

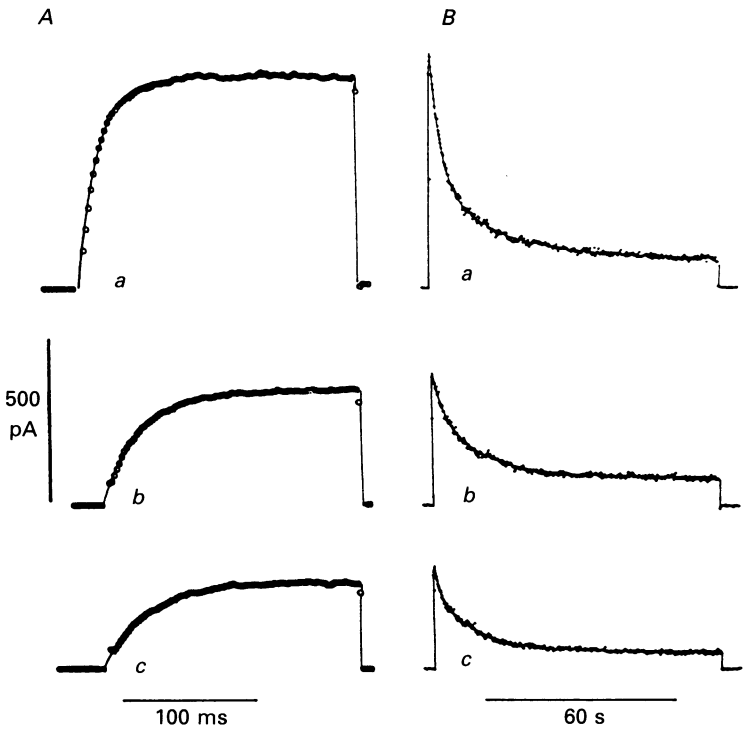

Fig. 14. Effect of 4-AP on activation and inactivation. Cell held at −60 mV and depolarized to 30 mV during either 200 ms (*A*) or 90 s (*B*) voltage jumps. Traces labelled *a* are responses in control solution (Table 1, solution A); traces labelled *b* and *c* are responses in 0·25 and 1 mM-4-AP respectively. In *A*, experimental values are shown at 2 ms intervals (omitting initial and final capacitative artifacts); fitted lines (t in ms):
for *a*, $695(1-\exp[(-t+1{\cdot}8)/14{\cdot}5])$ pA,
for *b*, $381(1-\exp[(-t+1{\cdot}8)/28{\cdot}7])$ pA,
for *c*, $289(1-\exp[(-t+2{\cdot}1)/33{\cdot}7])$ pA.
In *B*, fitted values at 1 s intervals are (t in s):
for *a*, $423\exp(-t/1{\cdot}7)+236\exp(-t/10)+87$ pA,
for *b*, $102\exp(-t/1{\cdot}7)+216\exp(-t/7{\cdot}1)+85$ pA,
for *c*, $95\exp(-t/0{\cdot}7)+191\exp(-t/10)+52$ pA.

Narahashi (1976), 4-AP can be seen to produce not only a concentration-dependent reduction in amplitude, of the outward current, but also a decrease in its activation rate. When the responses to prolonged depolarization were fitted according to eqn (23) (p. 137). It could be seen that the predominant effect of 4-AP was on the more rapidly inactivating component of the current. A summary of the effect of 4-AP on the amplitude of the outward current is given in Table 4.

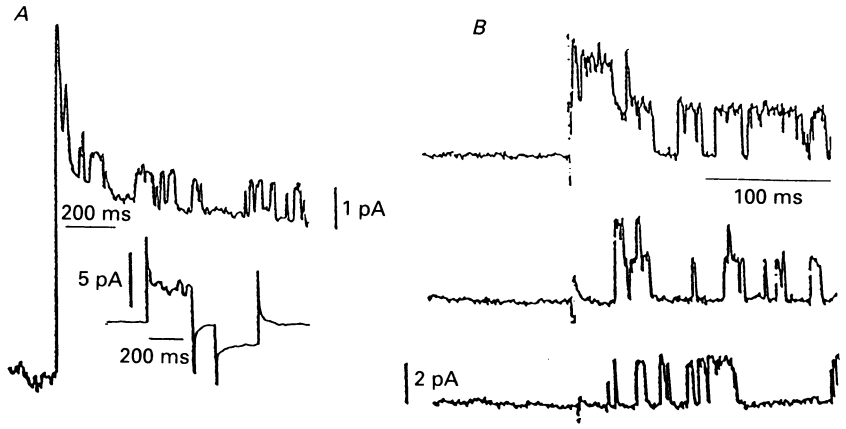

Fig. 15. Records of single-channel activity from cell-attached patches. *A*, uncorrected records from a patch held at resting potential and depolarized by 60 mV; shows responses to 60 mV depolarization (upward deflection) followed by 50 mV hyperpolarization at lower resolution. *B*, corrected records of outward currents from three different patches. In each case, the holding potential of patch was 20 mV hyperpolarized with respect to the resting potential; a depolarizing voltage-jump of 90 mV was then applied. Solution A (Table 1) was used in pipette and bath, but without tetrodotoxin. Records were filtered with an 8-pole Bessel filter, −3 dB at 1 kHz and sampled at intervals of 100 μs.

TABLE 4.

Concentration of 4-AP	Number of cells	Amplitude in 4-AP / Amplitude in control
0·25	5	0·58±0·11 (S.E.M.)
1·0	6	0·40±0·13 (S.E.M.)
4·0	1	0·32
10	1	0·32

Single-channel recording from cell-attached patches

Although a variety of different currents was seen (see e.g. Ginsborg *et al.* 1987), patches were usually quiescent when the trans-patch potential was equal to, or hyperpolarized with respect to the resting potential; when they were depolarized, patches displayed channel activity as shown in Fig. 15. The single-channel currents were of relatively large and uniform amplitude and it seemed appropriate to investigate their properties in greater detail.

Single-channel conductance

The single-channel conductance was determined by measuring single-channel currents activated by depolarizations to different levels. In the experiment illustrated in Fig. 16, the patch was hyperpolarized by 20 mV for several seconds before each period of depolarization by 50–90 mV. The slope conductance derived from Fig. 16*B* was 20 pS. Similar results were obtained from twenty different patches, the slope conductances falling within the range of 15–25 pS. Values within the same range

have been reported for a number of cells including the squid axon (17·5 pS originally observed by Conti & Neher, 1980, and 20 pS more recently by Llano, Webb & Bezanilla, 1988), murine N1E-115 neuroblastoma cells (20–25 pS, Misler & Falke, 1985), human (Decoursey *et al.* 1984) and murine lymphocytes (Lewis & Cahalan,

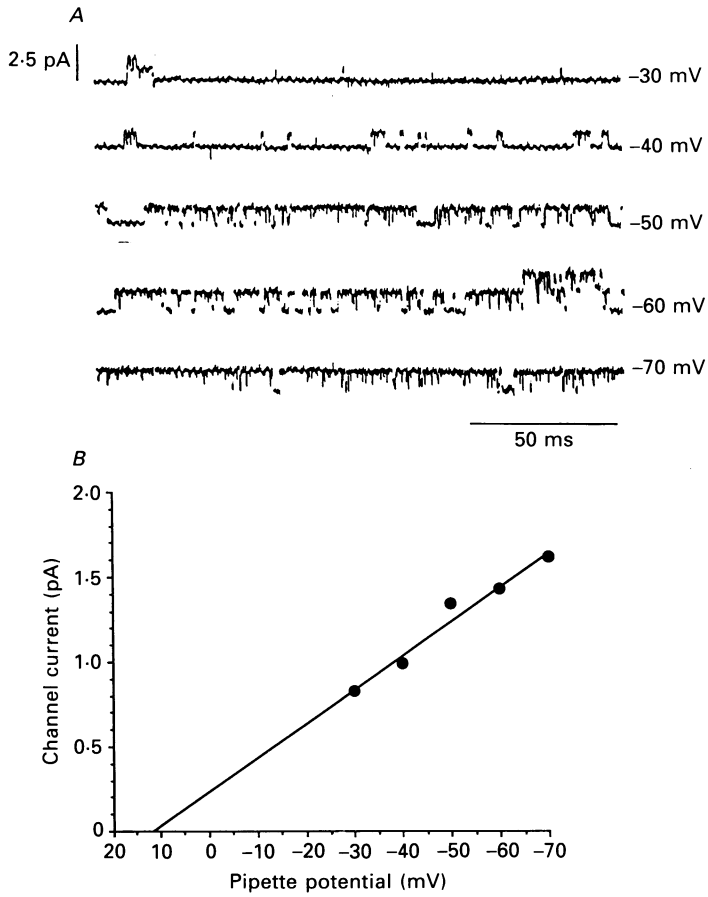

Fig. 16. Effect of membrane potential on single-channel currents. *A*, records are from the same patch which was first hyperpolarized by 20 mV for a few seconds and then depolarized by 50 mV to 90 mV, as indicated by values of final pipette potential given with each trace. *B*, plot of amplitude of channel current against pipette potential. Solution A (Table 1) was used in pipette and bath, but without tetrodotoxin. Records were filtered with an 8-pole Bessel filter, −3 dB at 1 kHz and sampled at intervals of 100 μs.

1988) (16–18 pS), *Xenopus* cultured spinal neurones (21 pS, Harris, Henderson & Spitzer, 1988, Fig. 3), cultured mouse peritoneal macrophages (16 pS, Ypey & Clapham, 1984), and cultured rat hippocampal neurones (15–20 pS, Rogawski, 1986). However, not all delayed rectifier channels have conductances close to 20 pS. Stansfeld & Feltz (1988) report values from 5 to 10 pS for dorsal root ganglion cells and Ypey, Ravesloot, Buisman & Nijweide (1988) values of the order of 100 pS for embryonic chick osteoblasts; (see Castle, Haylett & Jenkinson, 1989 for review).

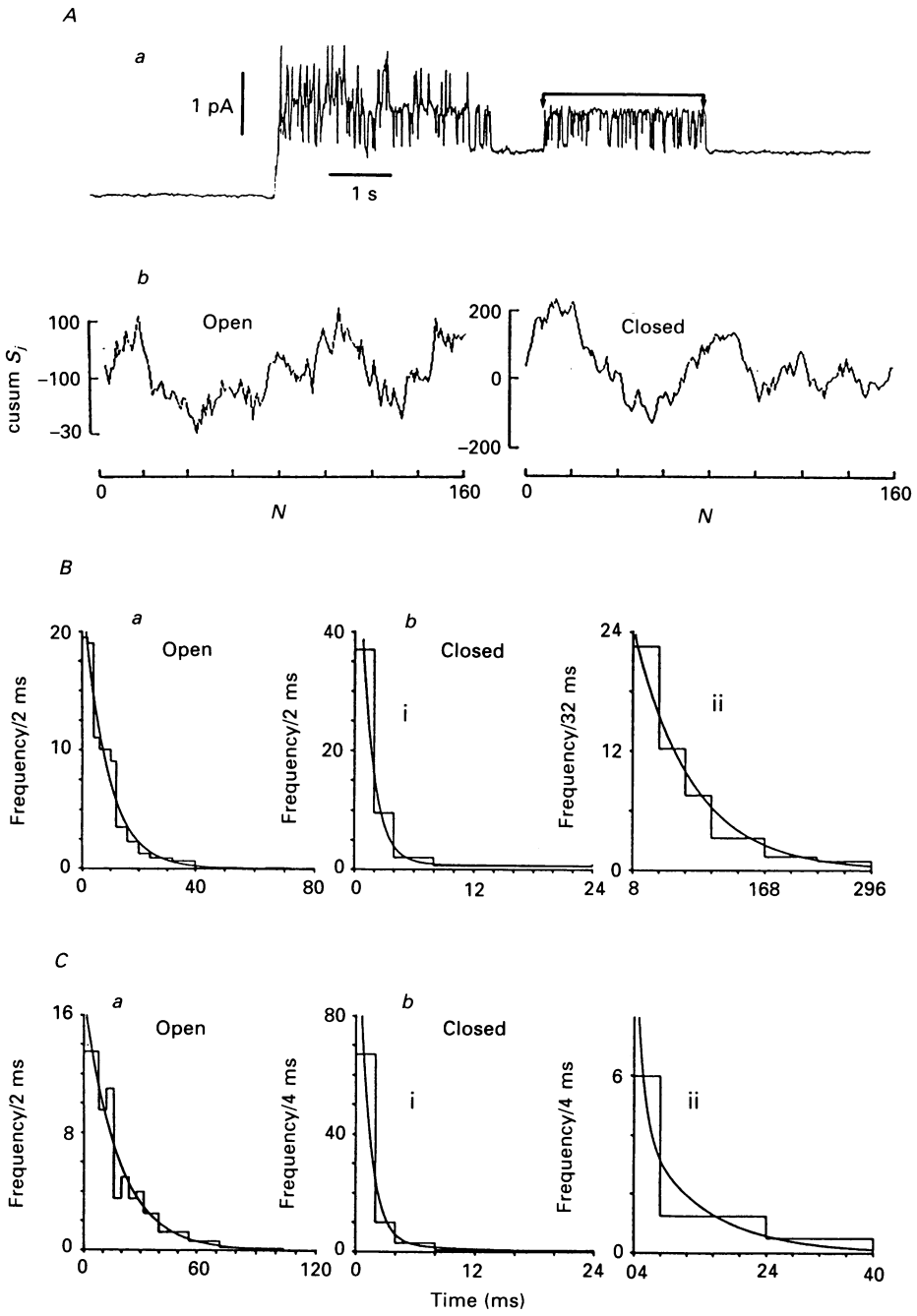

Fig. 17. Probability density functions of open and closed intervals (PDFs). *A*, selection of data: isolated cluster of single-channel activity (indicated by bar) tested for stationarity by cusum method (see text). Records were filtered with an 8-pole Bessel filter, −3 dB at 1 kHz and sampled at intervals of 100 μs. *B*, depolarizing voltage jump of 46 mV.

Kinetic analysis

When a patch was depolarized, and held at the depolarized level, single-channel behaviour which appeared to correspond to inactivation of whole-cell currents was observed. Thus the initial period of channel activity, which often contained simultaneous openings of several channels, was followed by alternate periods of 'silence' and of single openings. These were attributed to one and the same channel, for any given period, by analogy with the interpretation of the 'clusters of bursts' seen in patches of skeletal muscle endplates during desensitization by acetylcholine (Sakmann, Patlak & Neher, 1980). As illustrated in Fig. 17, this idea received some support from a cusum analysis (see Methods). A sample record is shown in Fig. 17*Aa* with the values of S_j (see eqn (1) plotted in Fig. 17*Ab* against N, the sequential number of either the opening (i) or closing (ii). It is immediately apparent that S_j does not deviate systematically from zero and the stationary behaviour of the events was confirmed by the significance test. Thus the probabilities of obtaining values of D_α (see eqn (3), for a random sequence, at least as large as those observed, for values of α of 9, 1 and 1/9, were 0·1, 0·93 and 1 for the open times, and 0·69, 1 and 0·94 for the closed times.

Probability density functions

The results from a patch depolarized by 46 and 82 mV were analysed in detail. Direct observations of the open probabilities for the 46 and 82 mV depolarizations were 0·26 and 0·89, respectively. The openings in response to the 46 mV depolarization were grouped into easily distinguishable bursts, the minimum interburst interval being 5 ms and the mean burst duration being 26 ms. From the PDFs illustrated in Fig. 17*B*, the mean values for the open times were 8·5 and 18 ms respectively for the 46 and 82 mV jumps (eqn (4), Methods). From the PDFs for the closed times (eqn (5), Methods) the values for a_s, τ_s, a_f and τ_f for the 46 and 82 mV jumps, were respectively: 0·41, 71 ms, 0·59 and 1·3 ms; 0·18, 9·9 ms, 0·82 and 1·1 ms. The predicted open probabilities (eqn (6), Methods) for the 46 and 82 mV jumps of 0·22 and 0·87 respectively are in reasonable agreement with those directly observed (0·26 and 0·89, see above). The predicted average burst duration for the 46 mV depolarization (eqn (17), Methods) of 22·6 ms is also in reasonable agreement with the directly observed value of 26 ms (see above).

A further test is provided by a comparison between the predicted and observed ratios of the steady (maximum) whole-cell currents, I_{max} say, evoked by stimuli corresponding to the 82 and 46 mV voltage jumps applied to the patch. If N is the total number of appropriate channels in the whole-cell membrane; g, the channel

---

a, histogram of open intervals in the range 0–80 ms with single exponential fit by maximum likelihood; time constant 8·5 ms. *b*, histograms of closed intervals in the ranges 0–24 ms (i) and 8–296 ms (ii); there was an additional interval of 593 ms. Superimposed fit (t in ms):

$$(0{\cdot}59/1{\cdot}26)\exp(-t/1{\cdot}26)+(0{\cdot}41/71{\cdot}4)\exp(-t/71{\cdot}4).$$

C, depolarizing voltage jump of 82 mV. *a*, histogram of open intervals in the range 0–120 ms; time constant, 18 ms. *b*, histograms of closed intervals in the ranges 0–24 ms (i) and 4–40 ms (ii). Superimposed fit (t in ms):

$$(0{\cdot}82/1{\cdot}13)\exp(-t/1{\cdot}13)+(0{\cdot}18/9{\cdot}9)\exp(-t/9{\cdot}9).$$

conductance; E_K, the potassium equilibrium potential; V, the potential to which the cell is depolarized; and $p_{1\infty}$, the equilibrium open probability at the potential V, then

$$I_{max} = Ngp_{1\infty}(V-E_K). \quad (24)$$

If the resting potential is taken as -40 mV and E_K as -70 mV, the predicted value of I_{max} (82)/I_{max} (46) is (0·87) (112)/(0·22) (76) = 5·8; if the resting potential is taken as -60 mV, the predicted ratio is 6·5. Experimentally, it was found that the whole-cell current ratio varied between 3·5 and 9 (three cells, see e.g. Fig. 7). Although the test is clearly not precise, the predictions and observations are not incompatible.

DISCUSSION

Sodium currents

The voltage-sensitive sodium currents evoked from the human neuroblastoma cell line IMR-32 are qualitatively similar to those that can be evoked from many other types of cell. The amplitudes are relatively small which partly reflects the small size of the cell, typically about 15 μm in diameter, and partly, presumably, a low channel density. Thus the maximum sodium conductance, that we have observed for the IMR-32 cell corresponds to about 2 mS/cm^2 which may be compared with values of 85 mS/cm^2 for the mouse neuroblastoma clone N1E-115 (Moolenaar & Spector, 1978) and 100 mS/cm^2 for rat sympathetic neurones (Belluzzi & Sacchi, 1986).

The method of estimating the time constants of activation and inactivation of the sodium current, τ_m and τ_h, allowed their determination over only a narrow voltage range and did not allow the separation of inactivation into slow and fast components. However, in so far as their values can be compared with other published results, τ_m and τ_h for IMR-32 neuroblastoma are within the range reported for other cells. Thus τ_m fell from 0·34 ms at -30 mV to 0·09 ms at 20 mV; the corresponding values for the rat sympathetic neurone, although at a slightly higher temperature, were 0·4 and 0·1 ms (Belluzzi & Sacchi, 1986). The value of τ_h for IMR-32 fell from 0·74 ms at -30 mV to 0·44 ms at $+20$ mV; the corresponding values for N1E-115, also estimated in a way which would not separate slow and fast inactivation, were 1 ms and 0·4 ms (Moolenaar & Spector, 1978).

Other features of activation and inactivation of the sodium current of IMR-32 cells are similar to those recently reported by Sah, Gibb & Gage (1988) for acutely dissociated hippocampal neurones. For both types of cell the maximum current occurs at a depolarization of -30 mV and with a time to peak, at this membrane potential, of about 1 ms. Also for both types of cell, about half the maximum conductance is inactivated at a holding potential around -80 mV and it requires depolarization to about -40 mV to activate half the available channels. The voltage sensitivity of activation is slightly greater for IMR-32 (k = 3·9 mV, eqn (18)) than for the hippocampal cells (k = 6·6 mV); for inactivation, the voltage sensitivities are almost identical.

Potassium currents

When depolarized, most cells generate a variety of outward potassium currents. These include transient voltage-dependent currents (I_A); a non-inactivating current (I_M); slowly inactivating voltage-dependent currents (I_K), and a number of different

calcium-dependent potassium currents. In the present investigation, it was found that the outward current of the undifferentiated IMR-32 cell was predominantly, if not exclusively, of the I_K variety (but see Gotti *et al.* 1987) as judged by the relatively depolarized holding potentials from which it could be evoked, by its slow rate of

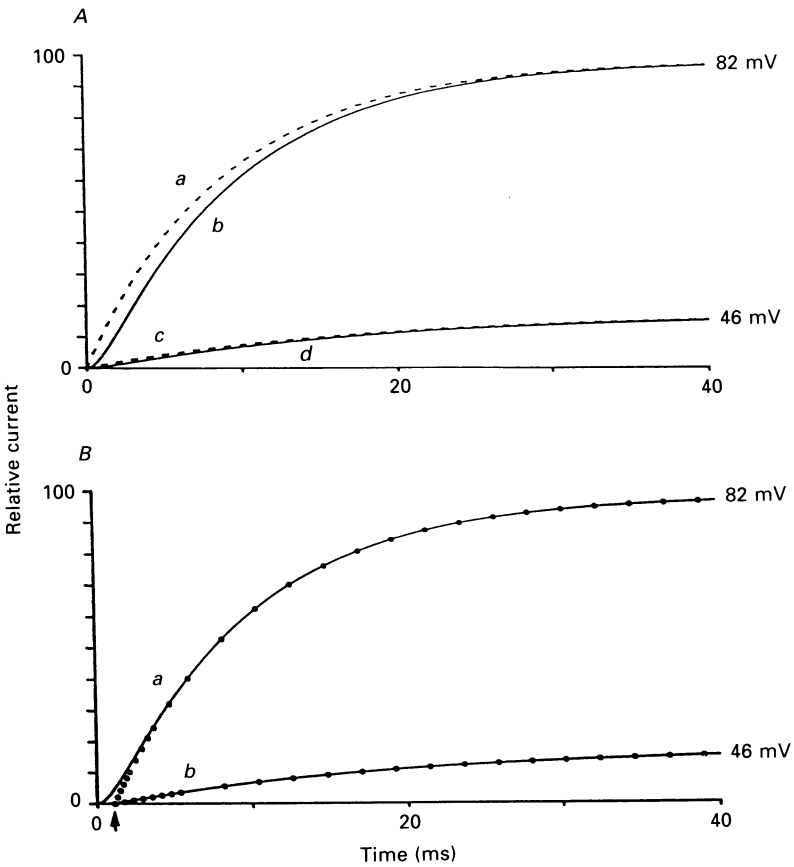

Fig. 18. Time course of rising phase of current predicted by PDFs according to the kinetic models COC and CCO. Ordinates are relative amplitudes of current. Upper curves correspond to a depolarizing jump of 82 mV and lower curves to 46 mV. In *A* the dashed lines correspond to the COC scheme. The continuous lines in both *A* and *B* correspond to CCO.
Aa (COC, 82 mV): $97{\cdot}4(1-0{\cdot}99\exp[-t/9{\cdot}0]-0{\cdot}01\exp[-t/1{\cdot}1])$.
Ab and *Ba* (CCO, 82 mV): $97{\cdot}4(1-1{\cdot}14\exp[-t/9{\cdot}0]+0{\cdot}14\exp[-t/1{\cdot}1])$.
Ac (COC, 46 mV): $16{\cdot}8(1-0{\cdot}99\exp[-t/17{\cdot}3]-0{\cdot}01\exp[-t/1{\cdot}2])$.
Ad and *Bb* (CCO, 46 mV): $16{\cdot}8(1-1{\cdot}07\exp[-t/17{\cdot}3]+0{\cdot}07\exp[-t/1{\cdot}2])$.
The circles in *Ba* correspond to $97{\cdot}4(1-\exp[(-t+1{\cdot}13)/9{\cdot}0])$, and in *Bb* to $16{\cdot}8(1-\exp[(-t+1{\cdot}18)/17{\cdot}3])$ (see text).

inactivation during prolonged depolarization, and by the effects of increasing the extracellular potassium concentration. It could be evoked in the virtual absence of calcium in the bathing solution and was thus not considered to be calcium dependent; it could be evoked in the virtual absence of anions and was therefore not

due to an influx of chloride ions. The absence of an inward current on hyperpolarization to −60 mV from a holding potential of −30 mV argues strongly against the existence of an I_M (see e.g. Brown, 1983, 1988) in IMR-32 cells.

Kinetic models

It seems highly likely that the '20 pS' channels described in the Results, which open on depolarization and have voltage-sensitive kinetics are those which underly the whole-cell currents. The kinetic models compatible with the single-channel PDFs presented in the Results, namely, closed ⇌ closed ⇌ open (C_2C_1O) and closed ⇌ open ⇌ closed (C_2OC_1) predict (eqns (12), (15) and (24); see legend for additional assumptions) the whole-cell currents illustrated in Fig. 18. It is clear that on account of the delayed rising phase of the current, the CCO model (continuous lines, Fig. 18*A*) provides a better fit to the observed form of the current. It is of further interest that, if the first few milliseconds are disregarded, the form of the empirical fit to the *observed* current (see eqn (21) $I(t) = I_{max}\{1-\exp[-(t-\delta t)/t_1]\}$, provides an excellent fit to the predicted currents (●, Fig. 18*B*) with values of δt (1·13 and 1·18, Fig. 18*B*) similar to those of the 'observed' delay terms (0·5–3·1 ms). Further qualitative support for the CCO model comes from the observation that two exponentially decaying components were required to describe the tail currents (see e.g. Fig. 10). The agreement between the experimental data and predictions based on the CCO model with the PDFs for the '20 pS' channels provides strong support for the idea that these channels underlie the whole-cell delayed rectifier current. As pointed out on p. 125, there was evidence for at least one extra term with time constant below 1 ms, corresponding to short-lived open and closed states that could not be properly resolved, in each of the PDFs. The additional terms to which they give rise will have very small time constants and would not affect the predictions based on the PDFs. Thus although the CCO model must be a simplification, it presumably represents an important part of the kinetic scheme (see e.g. Conti & Neher, 1980).

We thank Mr Greig Duncan and Miss Jackie O'Connell for preparing the cultures.

REFERENCES

Adams, P. R., Brown, D. A. & Constanti, A. (1982). M-Currents and other potassium currents in bullfrog sympathetic neurones. *Journal of Physiology* **330**, 537–572.

Belluzzi, O. & Sacchi, O. (1986). A quantitative description of the sodium current in the rat sympathetic neurone. *Journal of Physiology* **380**, 275–291.

Belluzzi, O., Sacchi, O. & Wanke, E. (1985*a*). A fast transient outward current in the rat sympathetic neurone studied under voltage-clamp conditions. *Journal of Physiology* **358**, 91–108.

Belluzzi, O., Sacchi, O. & Wanke, E. (1985*b*). Identification of delayed potassium and calcium currents in the rat sympathetic neurone under voltage clamp. *Journal of Physiology* **358**, 109–129.

Bezanilla, F. & Armstrong, C. M. (1977). Inactivation of the sodium channel I: sodium current experiments. *Journal of General Physiology* **70**, 549–566.

Brown, D. A. (1983). Slow cholinergic excitation – a mechanism for increasing neuronal excitability. *Trends in Neurosciences* **6**, 302–307.

Brown, D. A. (1988). M-Currents: an update. *Trends in Neurosciences* **11**, 294–299.

Cahalan, M. D., Chandy, K. G., DeCoursey, T. E. & Gupta, S. (1985). A voltage-gated potassium channel in human T lymphocytes. *Journal of Physiology* **358**, 197–237.

CARBONE, E., SHER, E. & CLEMENTI, F. (1990). Ca currents in human neuroblastoma IMR32 cells: kinetics, permeability and pharmacology. *Pflügers Archiv* **416**, 170–179.

CASTLE, N. A., HAYLETT, D. G. & JENKINSON, D. H. (1989). Toxins in the characterization of potassium channels. *Trends in Neurosciences* **12**, 59–65.

CLEMENTI, F., CABRINI, D., GOTTI, C. & SHER, E. (1986). Pharmacological characterization of cholinergic receptors in a human neuroblastoma cell line. *Journal of Neurochemistry* **47**, 291–297.

COLQUHOUN, D. & HAWKES, A. G. (1977). Relaxation and fluctuations of membrane currents that flow through drug-operated channels. *Proceedings of the Royal Society* B **199**, 231–262.

COLQUHOUN, D. & HAWKES, A. G. (1981). On the stochastic properties of single ion channels. *Proceedings of the Royal Society* B **211**, 205–235.

COLQUHOUN, D. & HAWKES, A. G. (1982). On the stochastic properties of bursts of single ion channel openings and clusters of bursts. *Philosophical Transactions of the Royal Society* B **300**, 1–59.

COLQUHOUN, D. & SIGWORTH, F. J. (1983). Fitting and statistical analysis of single-channel records. In *Single Channel Recording*, ed. SAKMANN, B. & NEHER, E., pp. 191–263. Plenum Press, New York and London.

CONNOR, J. A. & STEVENS, C. F. (1971). Voltage-clamp studies of a transient outward membrane current in gastropod neural somata. *Journal of Physiology* **213**, 21–30.

CONTI, F. & NEHER,E. (1980). Single channel recordings of K^+ currents in squid axons. *Nature* **285**, 140–143.

COOK, N. S. (1988). The pharmacology of potassium channels and their therapeutic potential. *Trends in Pharmacological Sciences* **9**, 21–28.

DECOURSEY, T. E., CHANDY, K. G., GUPTA, S. & CAHALAN, M. D. (1984). Voltage-gated K^+ channels in human T lymphocytes: a role in mitogenesis? *Nature* **307**, 465–468.

DUBOIS, J. M. (1981*a*). Simultaneous changes in the equilibrium potential and potassium conductance in voltage clamped Ranvier node in the frog. *Journal of Physiology* **318**, 279–295.

DUBOIS, J. M. (1981*b*). Evidence for existence of three types of potassium channels in the frog Ranvier node membrane. *Journal of Physiology* **318**, 297–316.

DUBOIS, J. M. (1983). Potassium currents in the frog node of ranvier. *Progress in Biophysics and Molecular Biology* **42**, 1–20.

GINSBORG, B. L., MARTIN, R. J. & PATMORE, L. (1987). On the electrical properties of a human neuroblastoma cell-line (IMR-32). *Journal of Physiology* **386**, 111*P*.

GLASEBY, C. A. & MARTIN, R. J. (1986). Exploratory and confirmatory plots of single-channel records. *Journal of Neuroscience Methods* **16**, 239–249.

GOTTI, C., SHER, E., CABRINI, D., BONDIOLOTTI, G., WANKE, E., MANCINELLI, E. & CLEMENTI, F. (1987). Cholinergic receptors, ion channels, neurotransmitter synthesis, and neurite outgrowth are independently regulated during the in vitro differentiation of a human neuroblastoma cell line. *Differentiation* **34**, 144–155.

GUPTA, M., NOTTER, M. D., FELTON, S. & GASH, D. M. (1985). Differentiation characteristics of human neuroblastoma cells in the presence of growth modulators and antimitotic drugs. *Developmental Brain Research* **19**, 21–29.

GUSTAFSSON, B., GALVAN, M., GRAFE, P. & WIGSTROM, H. (1982). A transient outward current in a mammalian central neurone blocked by 4-aminopyridine. *Nature* **299**, 252–254.

HAMILL, O. P., MARTY, A., NEHER, E., SAKMANN, B. & SIGWORTH, F. J. (1981). Improved patch-clamp techniques for high-resolution current recording from cells and cell-free membrane patches. *Pflügers Archiv* **391**, 85–100.

HARRIS, G. L., HENDERSON, L. P. & SPITZER, N. C. (1988). Changes in densities and kinetics of delayed rectifier potassium channels during neuronal differentiation. *Neuron* **1**, 739–750.

HILLE, B. (1984). Classical biophysics of the squid giant axon. *Ionic Channels of Excitable Membranes*, pp. 23–57. Sinauer Associates Inc., Sunderland, MA.

HODGKIN, A. L. & HUXLEY, A. F. (1952). A quantitative description of membrane current and its application to conduction and excitation in nerve. *Journal of Physiology* **117**, 500–544.

KAWA, K. (1988). Voltage-gated sodium and potassium currents and their variation in calcitonin-secreting cells of the chick. *Journal of Physiology* **399**, 93–113.

KONISHI, T. (1989). Voltage-dependent potassium channels in mouse Schwann cells. *Journal of Physiology* **411**, 115–130.

KOSTYUK, P. G., VESELOVSKY, N. S., FEDULOVA, S. A. & TSYNDRENKO, A. Y. (1981). Ionic currents in the somatic membrane of rat dorsal root ganglion neurons. III. Potassium currents. *Neuroscience* **6**, 2439–2445.

LEWIS, R. S. & CAHALAN, M. D. (1988). Subset-specific expression of potassium channels in developing murine T lymphocytes. *Science* **239**, 771–775.

LLANO, I., WEBB, C. K. & BEZANILLA, F. (1988). Potassium conductance of the squid giant axon. Single-channel studies. *Journal of General Physiology* **92**, 179–196.

MARTY, A. & NEHER, E. (1985). Potassium channels in cultured bovine adrenal chromaffin cells. *Journal of Physiology* **367**, 117–141.

MILLER, D. J. & SMITH, G. L. (1984). EGTA purity and the buffering of calcium ions in physiological solutions. *American Journal of Physiology* **246**, C160–166.

MISLER, S. & FALKE, L. (1985). Single 'delayed rectifier' potassium channel currents in neuroblastoma. *Biophysical Journal* **47**, 146a.

MOOLENAAR, W. H. & SPECTOR, I. (1978). Ionic currents in cultured mouse neuroblastoma cells under voltage-clamp conditions. *Journal of Physiology* **278**, 265–286.

NEHER, E. (1971). Two fast transient current components during voltage clamp on snail neurones. *Journal of General Physiology* **58**, 36–53.

ROGAWSKI, M. A. (1986). Single voltage-dependent potassium channels in cultured rat hippocampal neurons. *Journal of Neurophysiology* **56**, 481–493.

RUDY, B. (1988). Diversity and ubiquity of K channels. *Neuroscience* **25**, 729–749.

SAH, P., GIBB, A. J. & GAGE, P. W. (1988). Potassium current activated by depolarization of dissociated neurons from isolated hippocampal neurons. *Journal of General Physiology* **92**, 263–278.

SAKMANN, B., PATLAK, J. & NEHER, E. (1980). Single acetylcholine-activated channels show burst kinetics in the presence of desensitizing concentrations of agonist. *Nature* **286**, 71–73.

SAKMANN, B. & TRUBE, G. (1984). Conductance properties of single inwardly rectifying potassium channels in ventricular cells from guinea-pig heart. *Journal of Physiology* **347**, 641–657.

SHER, E., GOTTI, C., PANDIELLA, A., MADEDDU, L. & CLEMENTI, F. (1988). Intracellular calcium homeostasis in a human neuroblastoma cell line: modulation by depolarization, cholinergic receptors, and α-latrotoxin. *Journal of Neurochemistry* **50**, 1708–1713.

STANSFELD, C. & FELTZ, A. (1988). Dendrotoxin-sensitive K^+ channels in dorsal root ganglion cells. *Neuroscience Letters* **93**, 49–55.

TUMILOWICZ, J. J., NICHOLS, W. W., CHOLEN, J. J. & GREENE, A. E. (1970). Definition of a continuous human cell line derived from neuroblastoma. *Cancer Research* **30**, 2110–2118.

YEH, J. Z., OXFORD, G. S., WU, C. H. & NARAHASHI, T. (1976). Dynamics of aminopyridine block of potassium channels in squid axon membrane. *Journal of General Physiology* **68**, 519–535.

YPEY, D. L. & CLAPHAM, D. E. (1984). Development of a delayed outward-rectifying K^+ conductance in cultured mouse peritoneal macrophages. *Proceedings of the National Academy of Sciences of the USA* **81**, 3083–3087.

YPEY, D. L., RAVESLOOT, J. H., BUISMAN, H. P. & NIJWEIDE, P. J. (1988). Voltage-activated ionic channels and conductances in embryonic chick osteoblast cultures. *Journal of Membrane Biology* **101**, 141–150.